# Enhanced Cellular Uptake Of Phenamil Through Inclusion Complex With Histidine Functionalized β-Cyclodextrin As Penetrative Osteoinductive Agent

Jahed, Vahid; Vasheghani-Farahani, Ebrahim; Bagheri, Fatemeh; Zarrabi, Ali; Fink, Trine; Lambertsen Larsen, Kim

*Published in:*
Nanomedicine

*DOI (link to publication from Publisher):*
10.2147/IJN.S221669



*Publication date:*
2019

*Document Version*
Publisher's PDF, also known as Version of record

International Journal of Nanomedicine

Dovepress
open access to scientific and medical research

Open Access Full Text Article

ORIGINAL RESEARCH

# Enhanced Cellular Uptake Of Phenamil Through Inclusion Complex With Histidine Functionalized β-Cyclodextrin As Penetrative Osteoinductive Agent

This article was published in the following Dove Press journal:
*International Journal of Nanomedicine*



Vahid Jahed[1]
Ebrahim Vasheghani-Farahani[1]
Fatemeh Bagheri[2]
Ali Zarrabi[3]
Trine Fink[4]
Kim Lambertsen Larsen[5]

[1]Biomedical Engineering Division, Faculty of Chemical Engineering, Tarbiat Modares University, Tehran, Iran; [2]Department of Biotechnology, Faculty of Chemical Engineering, Tarbiat Modares University, Tehran, Iran; [3]Sabanci University Nanotechnology Research and Application Center (SUNUM), Tuzla 34956, Istanbul, Turkey; [4]Department of Health Science and Technology, Faculty of Health, Aalborg University, Aalborg, Denmark; [5]Department of Chemistry and Bioscience, Faculty of Chemistry, Aalborg University, Aalborg, Denmark

**Background:** Phenamil (PH) is a small molecule that induces bone formation through upregulation of the *TRB3* gene in the bone-regeneration process. β-Cyclodextrins (βCDs) with hydrophilic surfaces and a relatively hydrophobic cavity can form inclusion complexes with primarily hydrophobic small molecules such as PH, and increase their apparent solubility and dissolution rate. The hydrophilic surface of βCDs prevents their interaction with the hydrophobic lipids of the cell membrane for penetration. Therefore, binding of penetrative groups, such as lysine, arginine, and histidine (His), to βCDs for cell penetration is required.
**Aim:** The aim of this study was to investigate the effect of His-conjugated βCD on cellular uptake of PH for bone differentiation.
**Methods:** In this study, His-βCDs were synthesized and used to prepare an inclusion complex of His-βCD-PH. A hydroxypropyl–βCD-PH (HP-βCD-PH) inclusion complex for increasing PH solubility without a penetrative group was prepared for comparison. 3-D geometry of βCD derivatives and PH-inclusion complexes was investigated by Fourier-transform infrared spectroscopy and molecular docking. Alizarin red staining and real-time PCR were performed to compare bone differentiation of His-βCD-PH and HP-βCD-PH.
**Results:** The results suggested that the benzene ring of PH was inserted into the wide side of both His-βCD and HP-βCD. Alizarin red staining at 14 days postculture in the presence of His-βCD-PH at total concentration of 50 μM for PH showed that bone-matrix mineralization increased significantly compared with free PH and HP-βCD-PH. Real-time PCR confirmed this result, and showed gene expression increased significantly (*OPN* 1.84-fold, *OCN* 1.69-fold) when stem cells were cultured with His-βCD-PH.
**Conclusion:** The overall results indicated that His-βCD-PH is a promising carrier for osteoinductive PH with possible penetration ability and sustained release that reduces BMP2 consumption for differentiation of mesenchymal stem cells to bone tissue.
**Keywords:** phenamil, β-cyclodextrin, inclusion complex, histidine, cell penetration, bone regeneration

Correspondence: Ebrahim Vasheghani-Farahani
Biomedical Engineering Division, Faculty of Chemical Engineering, Tarbiat Modares University, Jalal ale Ahmad Highway, P.O. Box 14115-114, Tehran, Iran
Tel +98 21 8288 3338
Email evf@modares.ac.ir

Kim Lambertsen Larsen
Department of Chemistry and Bioscience, Faculty of Chemistry, Aalborg University, 7H Fredrik Bajers Vej — 1340, Aalborg 9220, Denmark
Tel +45 9 940 8521
Email kll@bio.aau.dk

## Introduction

Growth factors are polypeptides that through binding to cell-membrane receptors and signal guiding lead to changes in cellular behavior, such as differentiation and proliferation. For example, BMP2 is a growth factor secreted by osteoblasts and plays a key role in differentiating stem cells for bone regeneration. The use of BMP2 in clinical and

preclinical studies has been associated with successful bone formation.[1,2] Despite many benefits of BMP2, its widespread use is limited, due to the complex production process (gene cloning), high prices, low stability, and side effects when used in superphysiological concentrations.[3,4] As such, there is a need for an alternative with benefits similar to BMP2 for stimulating bone differentiation, but with fewer drawbacks. Low-molecular-weight nonpeptide small molecules with favorable features, such as high stability and low price, along with the ability to stimulate bone differentiation have been intensively studied in recent years.[1,2]

Phenamil (PH; Figure 1A) is an FDA-approved small molecule known as an amiloride diuretic drug that leads to osteogenesis by upregulating *TRB3* gene expression in bone signaling. Moreover, PH enhances the BMP-signaling pathway by decreasing expression of the SMURF1 protein and increasing the expression level of SMADs, which are essential transcriptional factors of the BMP pathway.[5–8] It has been reported that use of PH together with BMP2 could be effective in reducing the consumption of BMP2, thereby reducing costs and side effects while achieving the same level of ossification.[5,8,9] Unfortunately, despite all the useful features of PH, its poor aqueous solubility has limited its widespread use.[8] Furthermore, the positive differentiation effect of PH and its toxicity have shown that the therapeutic window is very narrow. In other words, PH is highly effective for bone formation at concentrations of 10 and 20 μM, but causes cell death with adverse effects on bone formation at higher concentrations.[10,11] Therefore, sustained delivery of PH within the desirable concentration range for bone formation is much required.

Cyclodextrins (CDs) are FDA-approved cyclic oligosaccharides with a hydrophilic outer surface and internal hydrophobic cavity that can form inclusion complexes with many hydrophobic molecules.[12,13] It has been proven that inclusion complexes of CDs have the potential to increase the apparent solubility and bioavailability of many drugs.[14–16] Among natural CDs, βCD (Figure 1B) is the most popular, because of its suitable cavity size for trapping many hydrophobic molecules.[14] Inclusion-complex formation with hydrophobic molecules not only increases their apparent solubility with reduced use of toxic solvents but also leads to sustained release of hydrophobic molecules with no burst effect. In aqueous solution, there is a dynamic equilibrium between the drug in the inclusion complex and free drug that is constantly being formed and dissociated.[17] Despite these benefits, noninvasive transfer of biomolecules like CDs through the cell membrane is restricted, due to their hydrophilic surface.[18] As such, to increase cellular uptake, CDs need to be modified to facilitate cell penetration.

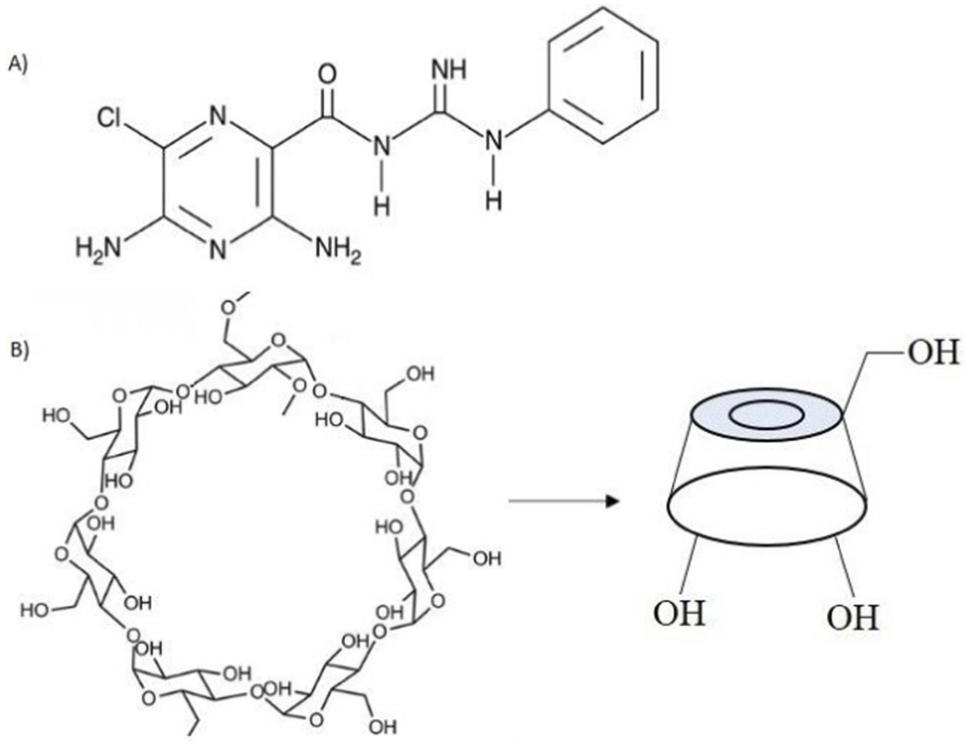


**Figure 1** Chemical structure of **A**) PH; **B**) βCD.

The cell membrane is composed primarily of anionic carbohydrates and lipids. Therefore, cationic molecules can interact electrostatically with the cell membrane and enter the cytoplasm through endocytosis or direct translocation. Lysine, arginine, and histidine (His) are cationic amino acids, among which His is a pH-sensitive amino acid with a higher positive charge than lysine and arginine at low pH.[19] The existence of a pH-sensitive domain on biomolecules helps their easy escape from endocytosis vesicles. Researchers have suggested a mechanism based on the His domain absorbs the proton's endosomal layer and results in increased osmotic pressure in the endosomal vesicle, endosomal membrane rupture, and consequent release of molecules in the cytoplasm (proton-sponge effect).[18,20] In one study, two groups of βCD derivatives (βCD-amine and βCD-His) were compared in terms of cell permeability. It was proved that His groups increased the penetration of CD into cells rather than amine groups.[21] In other studies, biomolecules attached to the His-rich chain for gene transfer exhibited high transfection efficiency[22] and functionalized αCD with His resulted in increased gene-transfer rates than non-His groups.[23]

The purpose of the present study was to investigate the induction efficiency of His-conjugated βCD-PH inclusion complexes on bone differentiation. Selective cationic His-functionalized βCD (His-βCD) was synthesized as a cell-penetration enhancer, and its effect on the solubility of PH was investigated in an aqueous medium. Then, inclusion complexes of His-βCD-PH and highly soluble hydroxypropyl–βCD-PH (HP-βCD-PH) were prepared and mesenchymal stem cell (MSC) differentiation from bone tissue in the presence of these inclusion complexes and BMP2 compared with that of free PH. Molecular dynamics were assessed to elucidate the 3-D geometry of the inclusion complexes.

# Methods

## Materials

βCD and HP-βCD (molecular weight 1,541.6 Da) were obtained from Wacker (Burghausen, Germany). Boc-His-OH, PH methanesulfonate, and all chemicals used for synthesis of βCD derivatives were purchased from Sigma-Aldrich. BMP2 growth factor was obtained from Thermo Fisher Scientific.

## His-βCD Synthesis

To prepare His-βCD, a previous method with a few modifications was used.[24] Figure 2 shows the synthesis procedure and structure of His-βCD. According to the procedure for selective His binding to 6-OH of βCD, at first 6-deoxy-amine-βCD (amine-βCD) was prepared. After attaching amine to the 6-OH, a covalent bond between the amine group from amine-βCD and the carboxyl group of His was established. For His-βCD preparation, a covalent bond of phenylalanine to amine-βCD was inspired.[25] Briefly, 66 mg Boc-His-OH (0.2 mmoL) and 80 mg *N*-hydroxybenzotriazole (0.4 mmol) were dissolved in 5 mL anhydrous *N,N*-dimethylformamide. Then, the solution was cooled to 0°C and 100 mg *N,N*-dicyclohexylcarbodiimide (0.4 mmol) was

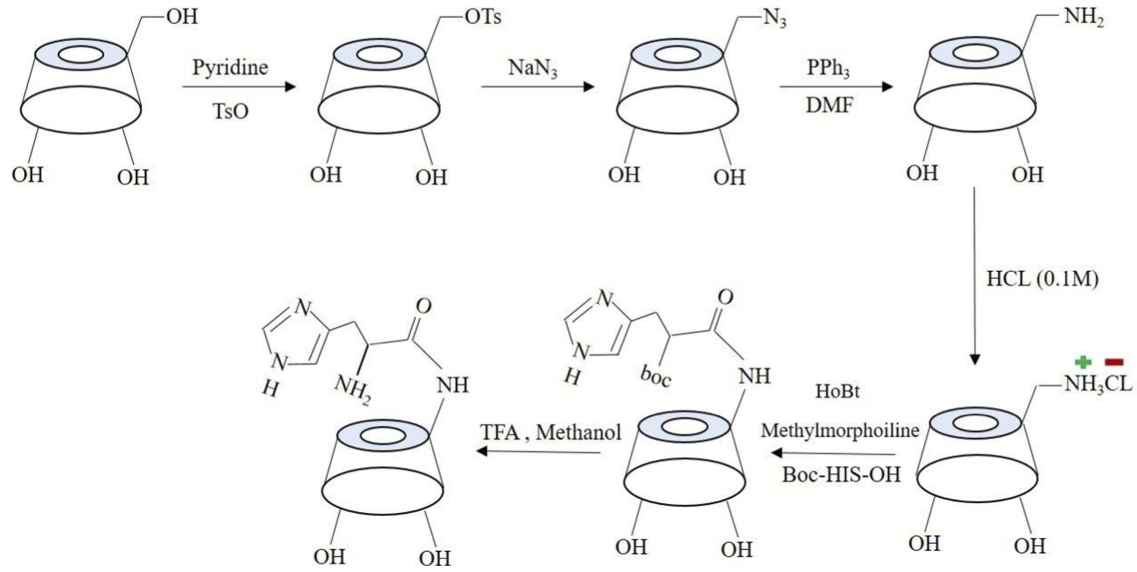


**Figure 2** Schematic of His-βCD preparation.

added and stirred at 0°C for 1 hour (400 rpm), followed by 4 hours (400 rpm) at room temperature to precipitate the by-product dicyclourea. Then, 260 mg 6-deoxy-amine-βCD and 120 µL ethylmorpholine suspension in 5 mL dimethylformamide were added to the reaction mixture and stirred at 40°C without a cap overnight. To ensure the end of the reaction, thin-layer chromatography (TLC) plates were prepared after 3, 5, and 7 hours. Then, dicyclohexylurea was filtered off to obtain oil-like liquid under reduced pressure and 50 mL acetone was added for product precipitation. The precipitate was washed with acetone twice and dried under high vacuum to obtain off-white powder (0.285 g, 87%). To remove the Boc group, the obtained powder was first dissolved in 2 mL trifluoroacetic acid and stirred. After 1 hour, to remove the acid, the resulting solution was washed with methanol several times, followed by solvent removal with a rotary evaporator and then freeze-dried to obtain the final product, which was characterized by $^{1}H$ nuclear magnetic resonance (NMR) and Fourier-transform infrared (FTIR) spectroscopy.

## Characterization

### Fourier-Transform Infrared Spectroscopy

FTIR spectra of all samples were recorded using FTIR spectrometry (Tensor II) equipped with a diamond attenuated total reflection (ATR) accessory. All transmittance spectra were generated by placing specific amounts of powder (air background) or liquid drops (liquid background) on the tip of the ATR. Data were obtained between 4,000 $cm^{-1}$ and 500 $cm^{-1}$ at 4 $cm^{-1}$ scanning speed with 64 scans.

### Hydrogen Nuclear Magnetic Resonance Analysis

All NMR spectra to characterize selective reaction of primary alcohol were recorded in DMSO-$d_6$ and the rest recorded in $D_2O$ using a Bruker Avance DRX 600 MHz. Parameters used during the NMR experiments were number of scans (32), relaxation delay (1 seconds) and pulse temperature (25°C).

### Dynamic Light Scattering And ζ-Potential

Dynamic light scattering (DLS) and ζ-potential of βCD derivatives with fixed concentrations at two pH values of 4.5 (related to early and late endosomes using 2-(*N*-morpholino)ethanesulfonic acid buffer) and 7.1 (related to cell environment using PBS) were measured with a particle-size analyzer (Malvern Zetasizer Nano ZS2000) based on quasielastic light scattering. Briefly, human adipose-derived SCs (hASCs) were cultured (passage 5) and then separated from the bottom of the plate, followed by centrifugation. Then, the supernatant was removed, followed by addition of 1 mL PBS and ζ-potential was recorded immediately.

## His-βCD-PH And HP-βCD-PH Inclusion-Complex Preparation

PH (1 mg) was added to aqueous solution containing various concentrations (0–10 mM) of βCD derivatives (His-βCD and HP-βCD) separately. The mixture was stirred for 48 hours to reach equilibrium at 37°C. After that, the mixture was centrifuged for 10 minutes at 3,000 rpm and the resulting supernatant was filtered with a 0.45 µm Phenex-RC (Phenomenex). Solid phases (undissolved PH) were collected and dried in an oven at 35°C for 2 days. $[PH]_T$ was obtained by ultraviolet absorbance at 289 and 365 nm with ultraviolet spectrophotometry. Also, HPLC (Kinetex $C_{18}$ column, 150×4.6 mm, 5 µm; Alltech) analysis was performed to measure the amount of CD derivatives and inclusion-complex components.

## Molecular Docking

Molecular docking was performed to elucidate the 3-D geometry of βCD derivatives and PH inclusion complex in aqueous medium using Schrödinger 2018 software. An amber force field was used in Polak–Ribière conjugate gradient–energy minimization of βCD derivatives and PH. Docking using Maestro Glide 11.8 was performed with the centroid of βCD derivatives to center the enclosing box as docking space. Glide score ($G_{score}$) and the most probable complexation for one minimized structure of βCD derivatives and PH, assuming 1:1 interaction, were recorded to compare the binding affinity of PH with the βCD derivatives.

## Cell Culture

hASCs were isolated from adipose tissue of a patient undergoing elective liposuction following the established procedure in the literature.[26] Cells were cultured in growth and proliferation αMEM (Sigma-Aldrich) supplemented with 10% FBS, 1% penicillin–streptomycin (100 U/mL), and 1% glutamic acid and incubated in a humidified 5% $CO_2$ atmosphere at 37°C. The cells were used for further experiments at passage 3.

## Cell-Cytotoxicity Assays

The viability of hASCs (at passages 5–6) was determined using MTT assays. Briefly, SCs were plated at a density of $8\times10^3$ cells/well and incubated for 24 hours. Then, the medium was exchanged with test solutions of PH at different concentrations (10, 20, 30, 40, and 50 μM) as well as βCD derivatives in the presence and absence of PH at specific concentrations (βCD-derivative concentrations were calculated from HPLC). After 24 hours, MTT solution (12 mM in PBS) was prepared and diluted (1:5) with fresh αMEM without FBS, added to each well, and then incubated for 3 hours at 37°C. After incubation, 100 μL DMSO was added to each well to dissolve formazan crystals, and then absorbance was recorded at 570 nm. The results were compared with those of untreated cells to obtain cell viability.

## Alizarin Red Staining

Alizarin red staining was performed to determine calcium deposition. Osteogenic differentiation medium supplemented with 0.05 mM L-ascorbic acid (Sigma-Aldrich), 10 mM glycerolphosphate disodium (Sigma-Aldrich), 100 nM dexamethasone (Sigma-Aldrich), and BMP2 (100 ng) was used to culture hASCs in the presence of test solutions. After 14 days, cells were fixed in 4% paraformaldehyde for 10 minutes and then washed with PBS twice and incubated in 2% Alizarin red stain solution for 5 minutes at 25°C. After that, all wells were washed gently five to six times with Milli-Q water to remove excess staining agent. Calcium-deposition images on the plate were taken and then red-stained samples were observed with an Olympus BX51 microscope. Also, quantitative calcium levels were determined using a previously established method.[27]

## Real-Time Polymerase Chain Reaction

hASCs were seeded on a 12-well plate at a density of $2\times10^5$ cells/well and incubated overnight. Cells were cultured for 14 days in osteogenic differentiation medium including test solution, and the medium was exchanged twice with a fresh one after 5 and 10 days. Then, total RNA was isolated with an RNeasy minikit (Bio-Rad) according to the manufacturer's protocol. Then, cDNA was synthesized from extracted RNA using an iScript advanced cDNA-synthesis kit (Bio-Rad). All primers used were produced by DNA Technology (Aarhus, Denmark). The total volume of each sample was 20 μL, and samples were analyzed in duplicate with a MyCycler real-time PCR system (Bio-Rad). The thermocycling program consisted of an initial step of 3 minutes at 95°C and 40 cycles of 15 seconds at 95°C and an annealing/extension temperature of 60°C for 30 seconds. Sequences of the primer sets were:

Osteocalcin (*OCN*) forward 5′-GAG CCC CAG TCC CCT ACC C-3′, reverse 5′-GCC TCC TGA AAG CCG ATG TG-3′

Osteopontin (*OPN*) forward 5′-TGA TGG CCG AGG TGA TAG TGT GGT-3′, reverse 5′-CCT GGG CAA CGG GGA TGG-3′

Peptidylprolyl isomerase A (*PPIA*) forward 5′-TCC TGG CAT CTT GTC CAT G-3′, reverse 5′-CCA TCC AAC CAC TCA GTC TTG-3′.

Fold-change gene-expression levels were recorded using the ΔΔCt method, in which the data were normalized with the expression level of PPIA.

## Statistical Analysis

Data were analyzed with ANOVA followed by Tukey–Kramer multiple-comparison tests using GraphPad Prism version 8.00 (GraphPad Software). $P<0.05$ was statistically significant. Values are expressed as means± SD.

# Results And Discussion

## Synthesis And Characterization Of His-βCD

One of the main goals of this study was the attachment of His penetrative group to the primary 6-OH of βCD, located on the primary side of βCD, allowing small molecules to enter the cavity of the βCD from the wider rim. Primary 6-OH of βCD functionalized with the amine group (amine-βCD) was prepared and then reacted with the carboxylic acid groups of His. All spectra assigned to amine-βCD synthesis from βCD were carried out in DMSO-$d_6$ to evaluate the selective reaction on the primary 6-OH of βCD. The results showed (Figure S1) that the $H_1$ (4.9 ppm) integration ratio to the secondary hydroxyl peaks (5.2 and 5.3 ppm) was constant (1:2) during the synthesis process from βCD to amine-βCD, while the $H_1$ ratio to the primary hydroxyl (4.2 ppm) changed. Therefore, it was proven that only the primary hydroxyl was functionalized with the amine group. Also, FTIR was performed to confirm the formation of the amine group. Figure 3A shows that the stretching peak at 2,110 $cm^{-1}$ attributed to the azide group in the azide-βCD spectrum disappeared when the azide group was converted to an amine group with a peak at 1,656 $cm^{-1}$ in the amine-

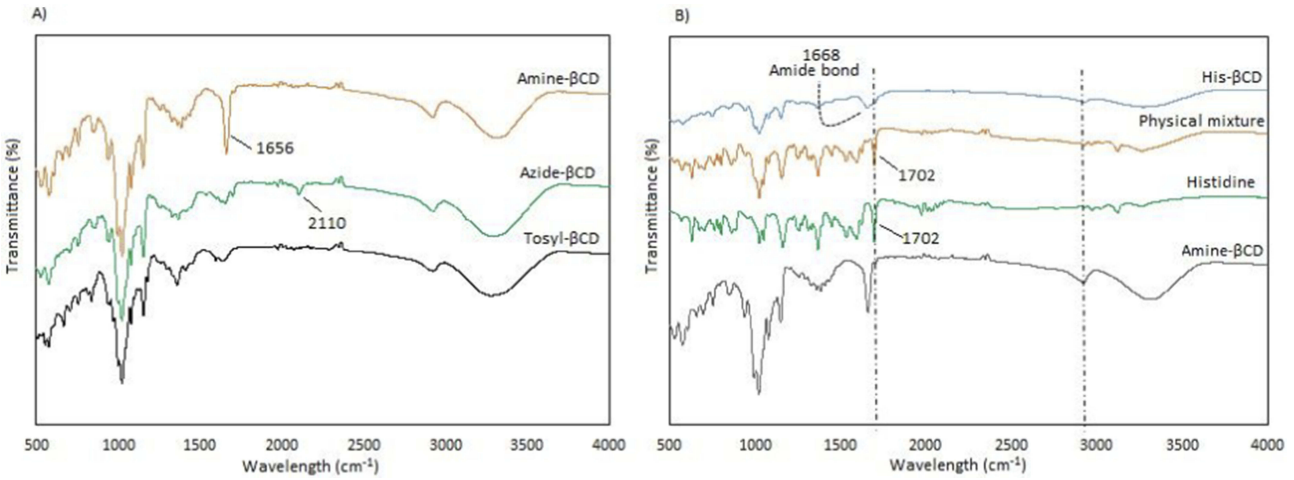


**Figure 3** FTIR spectra of **A**) intermediates during Amine-βCD, and **B**) His-βCD preparation.

βCD spectrum. After binding of the amine group to βCD had been ensured, His-βCD was characterized by TLC, $^1$H NMR, and FTIR analysis. TLC plates (Figure S2) showed that after 3 and 5 hours of reaction, amine-βCD reactant was still presented while it had completely reacted with His after 7 hours. FTIR spectra in Figure 3B show that the strong peak at 1,702 cm$^{-1}$, assigned to the C=O stretching of His, was present in the physical mixture but disappeared, and a new peak of covalent amide bond appeared at 1,668 cm$^{-1}$. As shown by $^1$H NMR spectra in Figure 4, three strong peaks of 7.26–8.6 ppm related to the imidazole ring of His appeared after its binding to amine-βCD. Also, FTIR spectra of Boc deprotection (Figure S3) indicated that the Boc group peak at 1,783 cm$^{-1}$ had completely disappeared, and the presence of the free amine group and the imidazole ring of His confirmed His-βCD synthesis.

## Inclusion-Complex Characterization

Higuchi and Connors presented equations based on CD solution and the amount of soluble drug from which the stability constant could be achieved.[28] The stability constant of βCD derivatives and PH inclusion complex represents a dynamic equilibrium between free PH and its complexed form. The linear stability constant ($K_{1:1}$) between βCD derivatives and PH was calculated by Equation 3, which was derived from Equations 1 and 2:

$$[PH] + [CD] \rightleftharpoons [PH - CD] \quad (1)$$

$$[PH]_T = [PH]_{Free} + [PH - CD] \quad (2)$$

$$K_{1:1} = \frac{S}{S_0(1-S)} = \frac{[PH-CD]}{[PH][CD]} = \frac{[PH]_T - [PH]_{Free}}{[PH]_{Free}[CD]} \quad (3)$$

where S and $S_0$ are slope of the phase-solubility diagram and the solubility of PH in the absence of βCD derivatives, respectively. $[PH]_{free}$ is the concentration of PH in the free state, and $[PH]_T$ refers to the total concentration of PH in the solution.

To obtain the stability constant ($K_{1:1}$) while assuming 1:1 βCD derivatives and PH inclusion–complex formation, the slope of the phase-solubility diagrams was obtained using Equation 3. As shown in Figure 5, the His-βCD-PH inclusion complex had a lower phase solubility–diagram slope than HP-βCD-PH, revealing that less HP-βCD was required to dissolve the same concentration of PH. This result revealed an $A_L$-type phase diagram for both βCD derivatives as well as His-βCD that could increase the solubility of PH in aqueous media linearly within the concentration range studied, but it proved less effective compared to HP-βCD. The apparent $K_{1:1}$ value of PH with HP-βCD and His-βCD was estimated to be $1.6\times10^3$ M$^{-1}$ and $7.29\times10^2$ M$^{-1,}$ respectively. In aqueous solution (eg, associated with the studied cell culture), a dynamic equilibrium between the free small molecules and the inclusion complex is established. This balance is substituted with a competitive displacement due to absorption of a drug by tissue, causing small molecules to release gradually.[29] In cell-culture medium, the small molecules are absorbed by the cells as a signal to change a dynamic balance, as long as all the small molecules in the inclusion complex are released as free components to be consumed by cells.

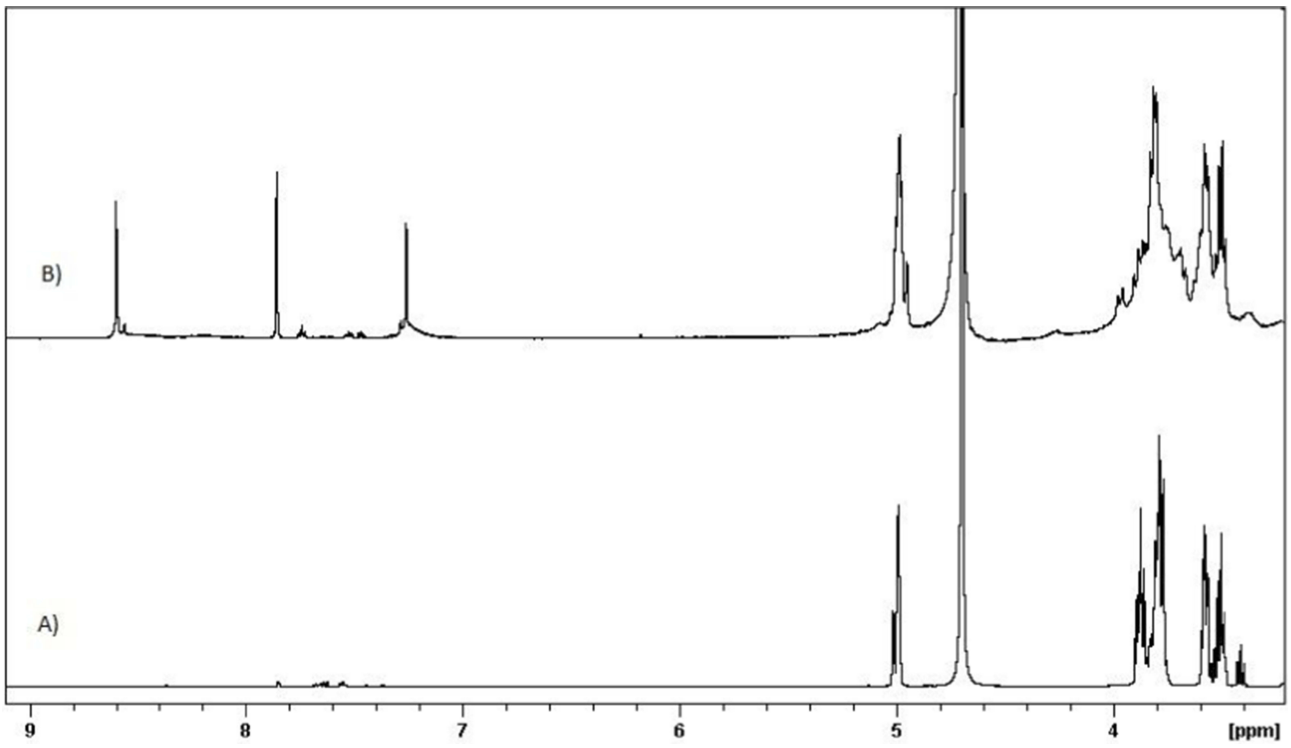


**Figure 4** H NMR spectra of **A**) Amine-βCD, **B**) His-βCD in $D_2O$.

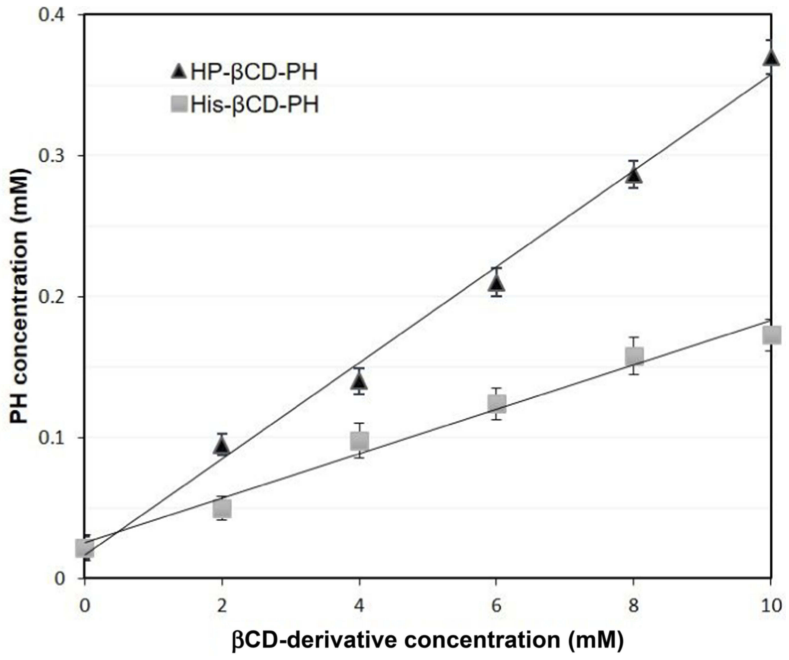


**Figure 5** Phase solubility diagram of βCD derivatives and PH at 37 °C. Data are expressed as the mean ± S.D. (n = 3).

As mentioned, 50 μM PH in DMSO was toxic and had a negative effect on bone formation. $[PH]_{Free}$ in His-βCD-PH and HP-βCD-PH inclusion complexes with 50 μM $[PH]_{T,}$ calculated by Equation 3, was 20.3 and 21.82 μM, respectively. In other words, the PH available in inclusion complexes was not released as long as free PH was consumed by MSCs. In these conditions, PH from His-βCD-PH and HP-βCD-PH inclusion complexes with 50 μM

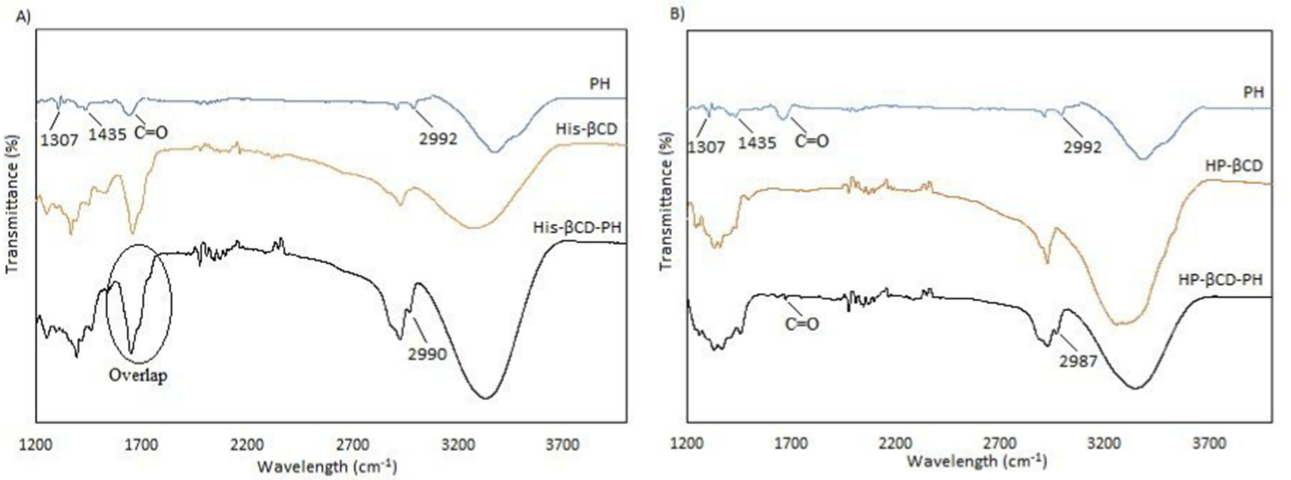


**Figure 6** FTIR spectra of **A**) His-βCD-PH, and **B**) HP-βCD-PH inclusion complex.

concentration was released gradually and allowed MSCs in the culture medium to be exposed to free PH with optimal concentration during differentiation to bone tissue.

Inclusion-complex formation was confirmed by FTIR. As shown in Figures 6, there were strong stretching vibration peaks related to the benzene ring attached to $NH_2$ of PH in the range of 1,300–1,450 $cm^{-1}$ and another peak at 2,992 $cm^{-1}$ assigned to the imidazole ring. When the inclusion complexes of His-βCD-PH and HP-βCD-PH were formed, the benzene-ring peak disappeared, while the imidazole ring peak remained (peak overlapping was seen in His-βCD between amide bond and C=O stretching peak of PH, marked by circle). This result indicated that the main reason for poor solubility of PH was the benzene ring completely disappeared after inclusion-complex formation. Moreover, $^1H$ NMR analysis was performed in $D_2O$ to verify the presence of PH in inclusion complexes. The weak peaks in the range of 7–8 that corresponded to the benzene ring of PH proved the presence of PH (Figure S4).

The size-distribution results of His-βCD-PH and HP-βCD-PH obtained by DLS are shown in Table 1. The size and polydispersity index of His-βCD-PH were less than those of HP-βCD-PH. ζ-Potential was also obtained to determine inclusion-complex surface charge and their potential interaction with negatively charged cell membrane. It should be noted that PH itself has a positive charge due to amine groups. The results in Table 1 show that the His-βCD-PH inclusion complex had a positive surface charge, while HP-βCD-PH was negative. This experiment was carried out at pH 4.5 (endosomal pH). The surface charge of His-βCD-PH was more positive with respect to its charge at pH 7.1, but surface charge of HP-βCD-PH was more negative. In a previous study, DLS analysis of histidinylated βCD showed narrow distribution and good stability at low concentration. The high positive charge of nanoparticles was also introduced as a reason for repulsion between the particles, as well as their stability in solution.[21] As a general consequence, the narrow size distribution of His-βCD-PH inclusion complex was due to repulsion of positively charged particles that reduced their aggregation, while HP-βCD-PH inclusion complexes tended to aggregate. On the other hand, the positive surface charge of His-βCD-PH may facilitate its electrostatic interaction with negatively charged cell membrane, as well as penetration into cells, with consequent rupture of the endosomal layer due to more positive charge at endosomal pH. Also, the negatively charged surface of

**Table 1** Size Distribution And ζ-potential Of PH Formulated With βCD Derivatives And hASCs

| | **Size Distribution (nm)** | **Polydispersity Index** | **ζ-Potential (pH 7.1)** | **ζ-Potential (pH 4.5)** |
|---|---|---|---|---|
| His-βCD-PH | 137±11 | 0.21 | 25±5 | 44±2 |
| HP-βCD-PH | 220±44 | 0.43 | −10±3 | −22±2 |
| hASCs in culture medium | — | — | −10±5 | — |

HP-βCD-PH inclusion complex cannot overcome the endosomal layer and escape by exocytosis, even if it enters the cell membrane through endocytosis.

Molecular docking on inclusion complexes between βCD derivatives and PH was performed to support phase solubility–diagram results. As shown in Figure 7, the benzene ring of PH was inserted into the βCD cavity in both His-βCD-PH and HP-βCD-PH. On the other hand, the lower $G_{score}$ (an empirical measure of how well a ligand fits in the binding pocket) showed stronger insertion of ligands to the CD.[30,31] $G_{scores}$ observed for PH binding with His-βCD and HP-βCD were −3.085 and −3.704 kJ $mol^{-1,}$ respectively. This result confirmed the phase-solubility diagram and a higher affinity for PH binding to HP-βCD compared with His-βCD-PH.

## Cell Treatment

As an osteoinductive agent, PH has optimal concentration where it has the lowest cytotoxicity on MSCs. To evaluate the optimal concentration of PH with the most positive effect on hASCs, MTT assays were run after 24 hours of incubation. As shown in Figure 8A, cell cytotoxicity increased with increased drug concentration dissolved in DMSO from 10 to 50 μM, and cell viability decreased to <80% at concentrations >20 μM. In this study, the optimum concentration of PH as an osteoinductive small molecule was 20 μM. As mentioned in the introduction, the suitable concentration has also been determined to be 20 μM. In previous studies, it was reported that PH at a concentration of 50 μM was toxic for MSCs, with adverse effects on bone formation,[10,11] which was confirmed in this study. Figure 8B shows that toxicity of βCD derivatives on hASCs was not significant and cell viability >90%. Moreover, the viability of hASCs treated with PH formulated using βCD derivatives at total concentration of 50 μM PH after 24 hours was investigated. In both cases (His-βCD-PH and HP-βCD-PH), significant toxicity was not observed at total concentration of 50 μM PH, which was probably due to the equilibrium between PH in the inclusion complex and the surrounding culture medium with a concentration close to optimal value.

## Osteogenesis

Extracellular matrix mineralization and quantitative calcium-level deposition were determined at 14 days postculture by Alizarin red staining. As shown in Figure 9A, in the presence of His-βCD-PH and HP-βCD-PH, matrix mineralization was increased clearly compared with the control. Free PH in DMSO at a concentration of 20 μM was selected as a control, since it induced the most positive osteogenesis

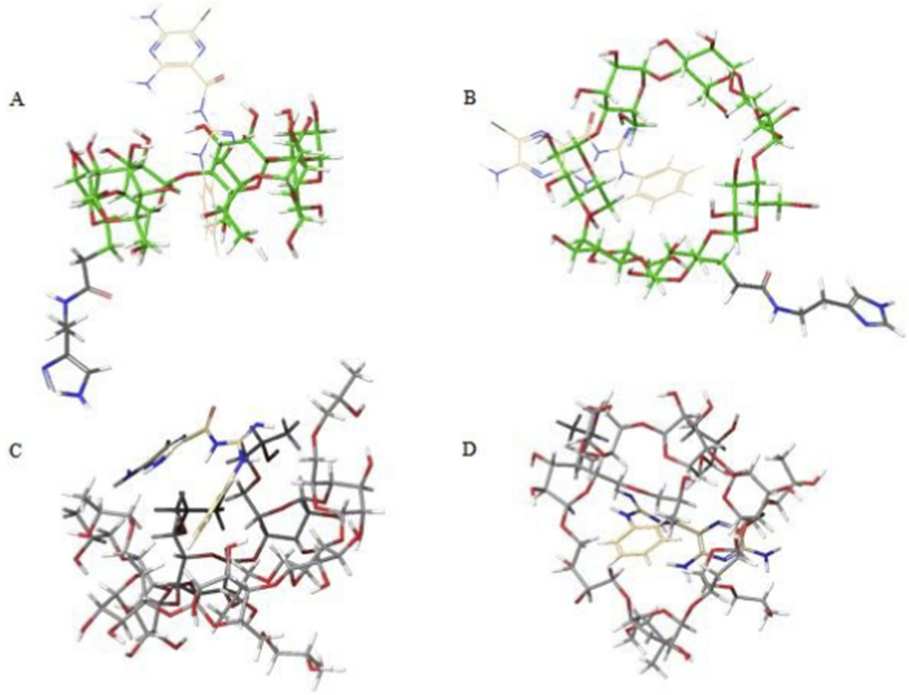


**Figure 7** Molecular docking of βCD derivatives and PH inclusion complex. **A**) His-βCD-PH (**B**: top view) and **C**) HP-βCD-PH (**D**: top view). Mono and random substitutions were designed for docking map based on $^{1}$H NMR and mass spectrometry for His-βCD and HP-βCD, respectively (Data are not shown here).

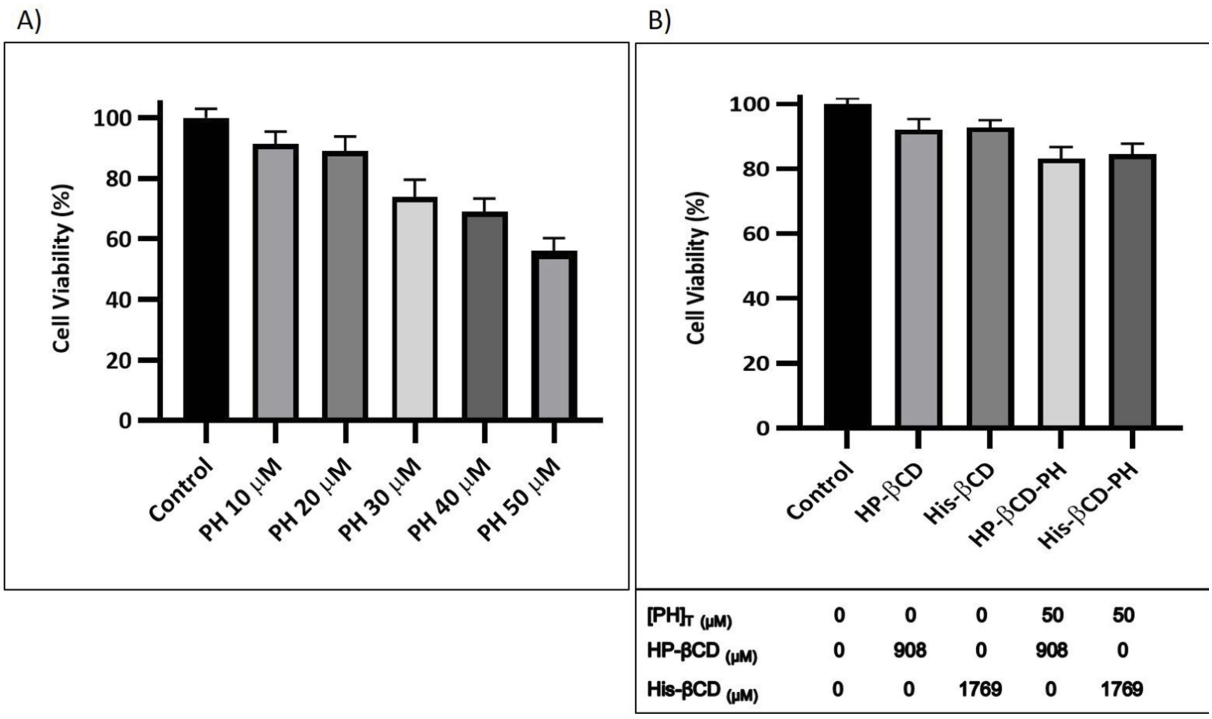


**Figure 8** Cell viability of **A**) PH in DMSO at different concentrations, **B**) βCD derivatives and corresponding inclusion complexes with PH after 24 hours. The $[PH]_T$ and $[CD]_T$ concentrations are shown below the diagram. Data are expressed as the mean ± S.D. (n = 3).

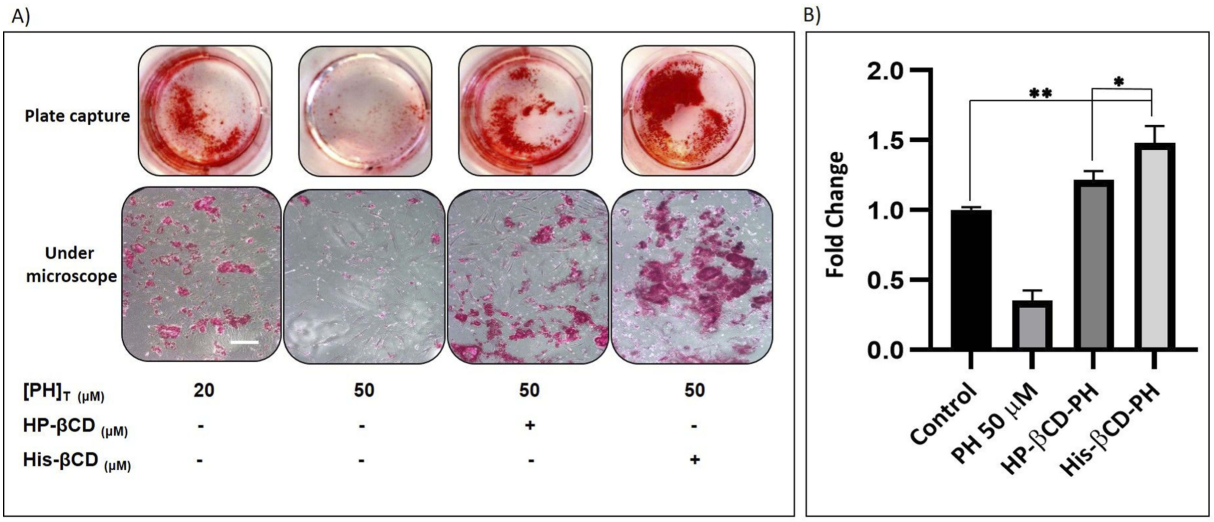


**Figure 9** Alizarin-red assay to bone matrix mineralization. **A**) Staining (Scale bar: 100 µm), and **B**) Quantitative calcium level deposition. Data are expressed as the mean ± S.D (n = 3). *p< 0.05, **p < 0.001).

effect for bone regeneration in a previous study.[5] It is postulated that sustained release of PH as a result of the equilibrium between PH in inclusion complexes of βCD derivatives and PH in cell-culture medium during differentiation had a significant positive effect on matrix mineralization. There was a difference between His-βCD-PH and HP-βCD-PH for matrix mineralization. Bone-matrix mineralization in the presence of His-βCD-PH was higher than that for HP-βCD-PH (Figure 9B). As shown in this figure, calcium-level deposition was significantly increased when hASCs were cultured with His-βCD-PH and HP-βCD-PH at 50 µM concentration compared with the control. The results indicated that in addition to increased solubility of PH by inclusion-complex formation, His conjugation as a

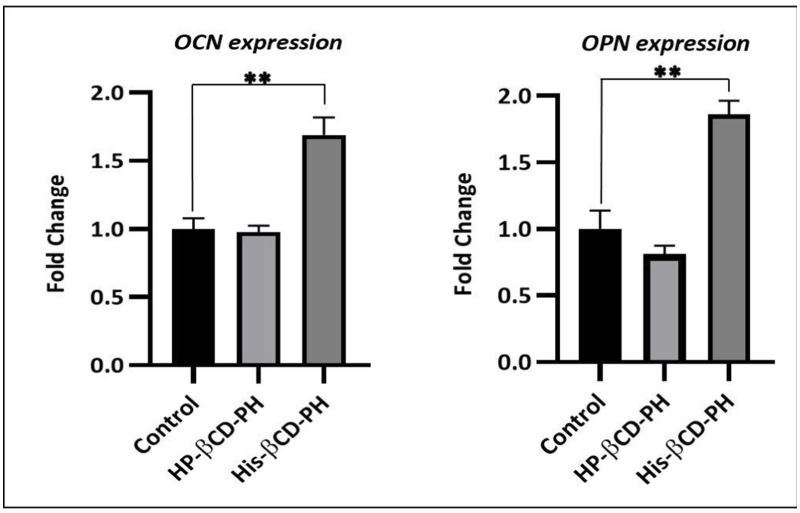


**Figure 10** Real-Time PCR to determine gene expression of bone delay markers. Control: PH at concentration of 20 μM in DMSO; PH in HP-βCD-PH and His-βCD-PH inclusion complexes at total concentration of 50 μM. Data are expressed as the mean ± S.D. (n = 3). **p < 0.001.

penetrative group contributed to increased bone mineralization. Electrostatic internalization of the His-βCD-PH inclusion complex by MSC membranes and their postendosomal escape followed by penetration into the nucleus might lead to better transfer of PH with consequent increase in bone-matrix mineralization. For detailed investigation on the effect of His-βCD-PH and HP-βCD-PH on hASCs for bone differentiation, real-time PCR was performed at 14 days postculture to investigate late bone-marker gene (*OCN* and *OPN*) expression. Figure 10 shows that gene expression increased significantly (*OPN* 1.84-fold, *OCN* 1.69-fold) when SCs were cultured with His-βCD-PH, but there was no significant change when they were cultured with HP-βCD-PH. This result revealed that HP-βCD could increase the solubility of PH, but it did not have a significant positive effect on delay in marker-gene expression, even though the total concentration of PH (not free PH) in the medium culture was higher than that of the control group. Generally, PH as a hydrophobic small molecule has good permeability through the hydrophobic cell membrane, while its cell permeability decreases when present in inclusion complexes. In addition, aggregation of HP-βCD at high concentrations may have prevented high transfection of PH into the nucleus compared with free PH (Figure 11). Therefore, the only advantage of HP-βCD is to load PH with sustained-release ability to avoid the toxic effect of PH at concentrations >20 μM. In a similar study, gene expression of HP-βCD and a random methyl-βCD (RM-βCD) inclusion complex with simvastatin (SV) as an osteoinductive agent (at tenfold concentration compared with free SV) was investigated. Results showed that the RM-βCD-SV inclusion complex increased ALP production and bone delay marker–gene expression significantly compared with HP-βCD-SV and free SV, while HP-βCD-SV did not show a significant difference from SV for osteogenesis. This difference was not explained, but RM-βCD-SV internalization was attributed to the hydrophobic methyl group of this complex.[32] Therefore, penetration of βCD-derivative inclusion complexes into cells with increased solubility of poorly soluble osteoinductive agents was considered responsible for the higher degree of differentiation of hASCs compared with the free agent. In another study, two nonglycerol-based histidylated cationic amphiphiles with only a single His head group were synthesized as a nonviral gene-transfection vector. The results showed that the carrier with a single His penetrative domain could transfer the gene to the nucleus properly and disturb the endosomal layer.[33]

BMP2 is an expensive osteoinductive growth factor compared with small molecules. To investigate the effect of PH on reducing BMP2 consumption, alizarin red staining was performed after 14 days of culture in osteogenic medium. A control group at a concentration of 20 μM free PH in DMSO and inclusion complex of His-βCD-PH at a total concentration of 50 μM ($[PH]_T$) containing $[PH]_{free}$ close to 20 μM with different amounts of BMP2 were used in culture medium. As shown in Figure 12, when BMP2 was reduced by half, bone-matrix mineralization in both groups decreased significantly, but the extent of such decrease for the

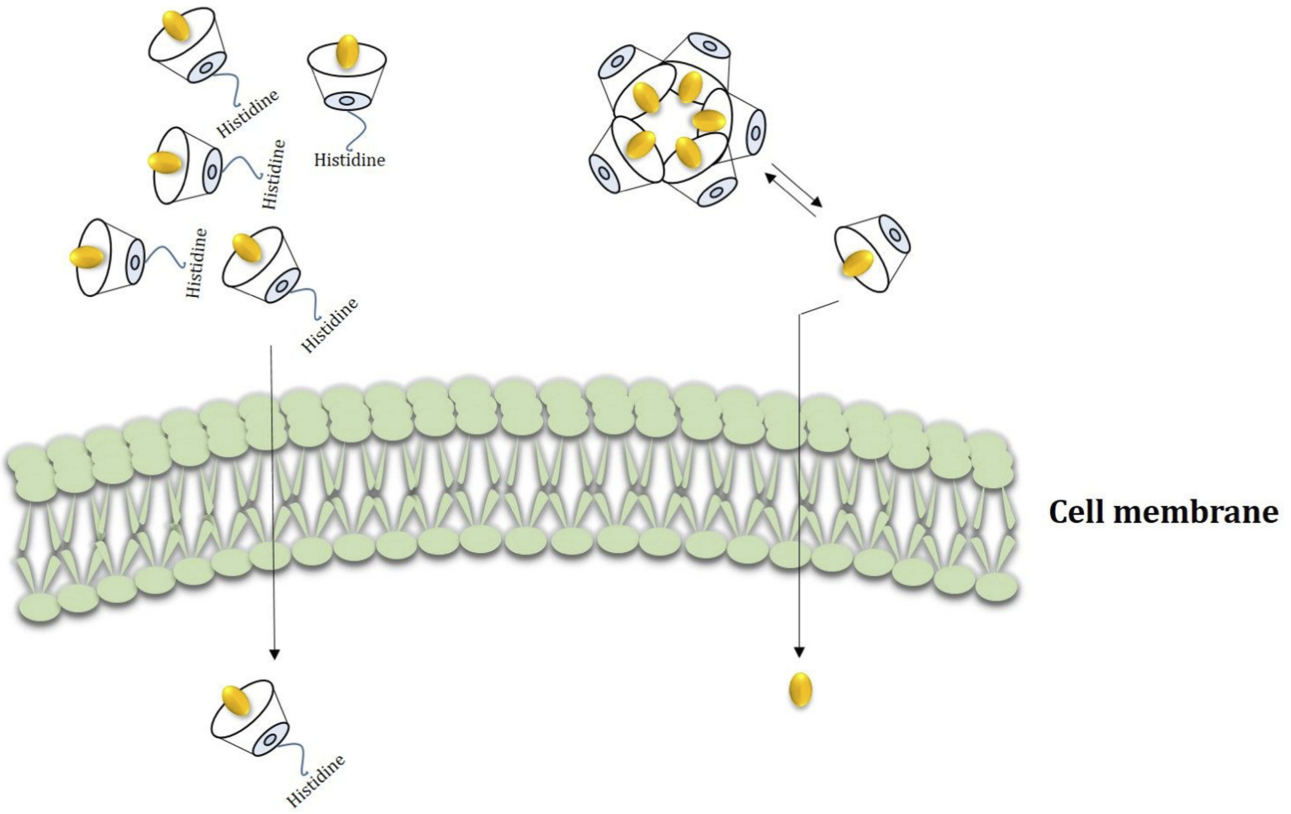


**Figure 11** Conceptual description of His-βCD-PH and HP-βCD-PH inclusion complexes transmittance across cell membrane. HP-βCD-PH aggregates constantly in cell culture and releases PH into cell membrane slowly but His-βCD-PH probably can penetrate into the cell membrane because of cationic amine group and hydrophobic affinity and release PH into cytoplasm and nucleus.

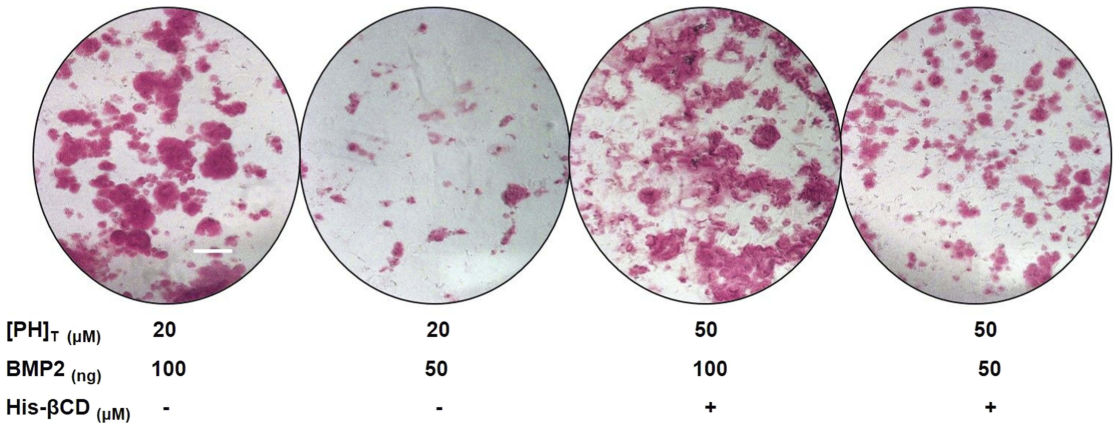


**Figure 12** The effect of His-βCD-PH inclusion complex and reduced BMP consumption on bone matrix mineralization obtained by Alizarin-red staining. Scale bar: 100 μm. Data are expressed as the mean ± S.D. (n = 3).

inclusion complex of His-βCD-PH was less than that of free PH at a concentration of 20 μM. We suggest that sustained release of PH from the inclusion complex of His-βCD-PH to culture medium helped to compensate the reduced amount of BMP2 consumption for differentiation of hASCs to bone tissue.

## Conclusion

Small molecules are important agents for differentiation of SCs because of their lower price and easier preparation with respect to growth factors. The main problem is their hydrophobic structure, which requires the use of toxic solvents, such as DMSO. Furthermore, most small molecules have an optimal

concentration at which they are most effective for cell differentiation with least cytotoxicity. The sustained release of small molecules at higher concentrations from suitable carriers provides desirable concentrations during the differentiation process. It is well established that βCD derivatives can increase the apparent solubility of small hydrophobic molecules and release them more slowly. In this study, inclusion complexes of His-βCD and PH as an osteoinductive agent at high concentrations were prepared. Conjugation of His to these inclusion complexes was also investigated. His-βCD not only increased the solubility of PH but also probably provided cell penetration and rupture of the endosomal layer with consequent transfer of PH to the nucleus for cell differentiation. The potential for sustained release of osteoinductive agents together with possible cell penetration makes this carrier very promising in bone tissue–engineering applications.

## Ethics Approval

The human adipose stem cells in this research were obtained from adipose tissue donated by a patient after written informed consent. The protocol was approved by the Regional Committee on Biomedical Research Ethics of Northern Jutland, Denmark (project VN 2005/54).

## Acknowledgments

We would like to show our gratitude to Helene Halkjær Jensen from the Department of Chemistry and Bioscience, Aalborg University for sharing her wisdom with us during this research.

## Disclosure

The authors report no conflicts of interest in this work.

## References

1. Balmayor ER. Targeted delivery as key for the success of small osteoinductive molecules. *Adv Drug Deliver Rev*. 2015;94(1):13–27. doi:10.1016/j.addr.2015.04.022
2. Agrawal V, Sinha M. A review on carrier system for bone morphogenetic protein-2. *J Biomed Mater Res*. 2016;105(4):904–925. doi:10.1002/jbm.b.33599
3. Liu XM, Wiswall AT, Rutledge JE, et al. Osteotropic β-cyclodextrin for local bone regeneration. *Biomaterials*. 2008;29(11):1686–1692. doi:10.1016/j.biomaterials.2007.12.023
4. Terauchi M, Inada T, Kanemaru T, et al. Potentiating bioactivity of BMP-2 by polyelectrolyte complexation with sulfonated polyrotaxanes to induce rapid bone regeneration in a mouse calvarial defect. *J Biomed Mater Res*. 2017;105(5):1355–1363. doi:10.1002/jbm.a.36016
5. Fan J, Im CS, Cui ZK, et al. Delivery of phenamil enhances BMP-2-induced osteogenic differentiation of adipose-derived stem cells and bone formation in calvarial defects. *Tissue Eng Pt A*. 2015;21(13–14):1–13. doi:10.1089/ten.tea.2014.0489
6. Park KW, Waki H, Kim WK, et al. The small molecule phenamil induces osteoblast differentiation and mineralization. *Mol Cell Biol*. 2009;29(14):3905–3914. doi:10.1128/MCB.00002-09
7. Fan J, Guo M, Im CS, et al. Enhanced mandibular bone repair by combined treatment of bone morphogenetic protein 2 and small-molecule phenamil. *Tissue Eng Pt A*. 2017;23(5–6):195–206. doi:10.1089/ten.tea.2016.0308
8. Cui ZK, Sun JA, Baljon JJ, et al. Simultaneous delivery of hydrophobic small molecules and sirna using sterosomes to direct mesenchymal stem cell differentiation for bone repair. *Acta Biomater*. 2017;58(1):214–224. doi:10.1016/j.actbio.2017.05.057
9. Fan J, Pi-Anfrun J, Guo M, et al. Small molecule-mediated tribbles homolog 3 promotes bone formation induced by bone morphogenetic protein-2. *Sci Rep-Uk*. 2017;7(1):7518–7526. doi:10.1038/s41598-017-07932-z
10. Lo K, Ulery BD, Kan HM, Ashe KM, Laurencin CT. Evaluating the feasibility of utilizing the small molecule phenamil as a novel biofactor for bone regenerative engineering. *J Tissue Eng Reg Med*. 2012;8(9):728–736. doi:10.1002/term.v8.9
11. Miszuk JM, Xu T, Yao Q, et al. Functionalization of PCL-3D electrospun nanofibrous scaffolds for improved BMP2-induced bone formation. *Appl Mater Today*. 2018;10(1):194–202. doi:10.1016/j.apmt.2017.12.004
12. Kurkov SV, Loftsson T. Cyclodextrins. *Int J Pharm*. 2013;453(1):167–180. doi:10.1016/j.ijpharm.2012.06.055
13. Loftsson T, Hreinsdottir D, Masson M. Evaluation of cyclodextrin solubilization of drugs. *Int J Pharm*. 2005;302(1–2):18–28. doi:10.1016/j.ijpharm.2005.05.042
14. Kashapov RR, Mamedov VA, Zhukova NA, et al. Controlling the binding of hydrophobic drugs with supramolecular assemblies of β-cyclodextrin. *Colloid Surface A*. 2017;527(1):55–62. doi:10.1016/j.colsurfa.2017.05.026
15. Sambasevam KP, Mohamad S, Sarih NM, Ismail NA. Synthesis and characterization of the inclusion complex of β-cyclodextrin and Azomethine. *Int J Mol Sci*. 2013;14(2):3671–3682. doi:10.3390/ijms14023671
16. Jahed V, Zarrabi A, Bordbar AK, et al. NMR (1H, ROESY) spectroscopic and molecular modelling investigations of supramolecular complex of β-cyclodextrin and curcumin. *Food Chem*. 2014;165(1):241–246. doi:10.1016/j.foodchem.2014.03.133
17. Jansook P, Ogawa N, Loftsson T. Cyclodextrins: structure, physicochemical properties and pharmaceutical applications. *Int J Pharm*. 2018;535(1–2):272–284. doi:10.1016/j.ijpharm.2017.11.018
18. Nguyen TV, Shin MC, Min KA, Huang Y, Oh E, Moon C. Cell-penetrating peptide-based non-invasive topical delivery systems. *J Pharm Invest*. 2018;48(1):77–87. doi:10.1007/s40005-017-0373-1
19. Iwasaki T, Tokuda Y, Kotake A, et al. Cellular uptake and *in vivo* distribution of polyhistidine peptides. *J Control Release*. 2015;210(1):15–24. doi:10.1016/j.jconrel.2015.05.268
20. Guidotti G, Brambilla L, Rossi D. Cell-penetrating peptides: from basic research to clinics. *Trends Pharmacol Sci*. 2017;38(4):406–424. doi:10.1016/j.tips.2017.01.003
21. Liu W, Zhang X, Wang R, Xu H, Chi B. Supramolecular assemblies of histidinylated β-cyclodextrin for enhanced oligopeptide delivery into osteoclast precursors. *J Biomater Sci-Polym E*. 2016;27(6):490–504. doi:10.1080/09205063.2016.1140612
22. Durzy_nska J, Przysiecka L, Nawrot R, et al. Viral and other cell-penetrating peptides as vectors of therapeutic agents in medicine. *J Pharmacol Exp Ther*. 2015;354(1):32–42. doi:10.1124/jpet.115.223305
23. Yang C, Li H, Goh SH, Li J. Cationic star polymers consisting of α-cyclodextrin core and oligoethylenimine arms as nonviral gene delivery vectors. *Biomaterials*. 2008;28(21):3245–3254. doi:10.1016/j.biomaterials.2007.03.033
24. Tang W, Choon S. Facile synthesis of mono-6-amino-6-deoxy-α-, β, γ-cyclodextrin hydrochlorides for molecular recognition, chiral separation and drug delivery. *Nat Protoc*. 2008;3(4):691–697. doi:10.1038/nprot.2008.37

25. Ashton PR, Koniger R, Stoddart JF. Amino acid derivatives of β-cyclodextrin. *J Org Chem*. 1996;61(3):903–908. doi:10.1021/jo951396d
26. Pilgard L, Lund P, Rassmusen GJ, Fink T, Zachar V. Comparative analysis of highly defined proteases for the isolation of adipose tissue-derived stem cells. *Reg Med*. 2008;3(5):705–715. doi:10.2217/17460751.3.5.705
27. Gregory CA, Gunn WG, Peister A, Prockop DJ. An Alizarin red-based assay of mineralization by adherent cells in culture: comparison with cetylpyridinium chloride extraction. *Anal Biochem*. 2004;329(1):77–84. doi:10.1016/j.ab.2004.02.002
28. Higuchi T, Connors KA. Phase solubility techniques. *Adv Anal Chem Instr*. 1965;4(1):117–212.
29. Stella VJ, Rao VM, Zannou EA, et al. Mechanisms of drug release from cyclodextrin complexes. *Adv Drug Deliver Rev*. 1999;36(1):3–16. doi:10.1016/S0169-409X(98)00052-0
30. Sameena Y, Sudha N, Murugesan G, et al. Isolation of Prunin from the fruit shell of Bixa orellana and the effect of β-cyclodextrin on its binding with calf thymus DNA. *Carbohydr Res*. 2013;356(1):46–51.
31. Sameena Y, Sudha N, Chandrasekaran S, Enoch IVMV. The role of encapsulation by β-cyclodextrin in the interaction of raloxifene with macromolecular targets: a study by spectroscopy and molecular modeling. *J Biol Phys*. 2014;40(1):347–367. doi:10.1007/s10867-014-9355-y
32. Terauchi M, Inada T, Tonegawa A, et al. Supramolecular inclusion complexation of simvastatin with methylated β-cyclodextrins for promoting osteogenic differentiation. *Inter J Biol Macromol*. 2016;93(1):1492–1498. doi:10.1016/j.ijbiomac.2016.01.114
33. Kumar VV, Pichon C, Refregiers M, Guerin B, Midoux P, Chaudhuri A. Single histidine residue in head-group region is sufficient to impart remarkable gene transfection properties to cationic lipids: evidence for histidine mediated membrane fusion at acidic pH. *Gene Ther*. 2003;10(15):1206–1215. doi:10.1038/sj.gt.3301979